

$Mn^{55}(d,\alpha)Cr^{53}$  studies, since the corresponding region of the alpha-particle spectrum was obscured by groups from contaminants.

While the good agreement between the values for the excited states in  $Cr^{53}$  obtained from the  $Mn^{55}(d,\alpha)$  and  $Cr^{52}(d,p)$  reactions provides a check on the correct assignment of the ground-state groups of these reactions, additional confirmation is obtained by comparing the  $Q$  value for the  $Mn^{55}(p,\alpha)Cr^{52}$  reaction calculated from the results reported here with that observed

experimentally.<sup>2</sup> This latter value is  $2.568 \pm 0.008$  Mev and is in agreement with the calculated one within the experimental errors. The present results on  $Cr^{53}$  are in substantial agreement with those reported by other workers.<sup>3,4</sup>

<sup>2</sup> Mazari, Buechner, and Sperduto, *Phys. Rev.* **107**, 1383 (1957).

<sup>3</sup> A. J. Elwyn and F. B. Schull, *Bull. Am. Phys. Soc. Ser. II*, **1**, 281 (1956).

<sup>4</sup> *Nuclear Level Schemes, A=40-A=92*, compiled by Way, King, McGinnis, and van Lieshout, Atomic Energy Commission Report TID-5300 (U. S. Government Printing Office, Washington, D. C., 1955).

## Steady-State Free Precession in Nuclear Magnetic Resonance\*

H. Y. CARR

*Department of Physics, Rutgers University, New Brunswick, New Jersey*

(Received August 4, 1958)

A steady-state free precession technique for observing nuclear magnetic resonance is described. A mathematical analysis is presented for certain special conditions, and initial experiments verifying the results of this analysis are reported. This technique provides two opportunities for improving the signal-to-noise ratio. First, it provides a mechanism, similar to that of the "spin echo," for eliminating the effect of the inhomogeneity of the magnetic field on signal strength. This permits the effective use of larger samples. In the second place it provides a steady-state signal which can be observed with a narrow-band detector. Under certain conditions the technique has a broad response as a function of frequency or field. The upper limit to the width of this response is determined by the electronic apparatus supplying the rf pulses rather than the magnet or the nuclear sample.

### I. INTRODUCTION

NUCLEAR magnetic resonance in condensed matter was first observed by Purcell, Torrey, and Pound<sup>1</sup> and by Bloch, Hansen, and Packard.<sup>2</sup> The experimental techniques used by these two groups<sup>3,4</sup> provide an output signal which can be related to the forced precession of a steady-state nuclear magnetic moment associated with the bulk sample. The precession is called forced because at the time the output signal is observed, the precession is determined not simply by the static magnetic field but also to a large extent by an additional component of the field oscillating near the resonance frequency. The net nuclear moment is considered in a steady-state because in periods of time equal to or shorter than the spin relaxation times it does not undergo changes in amplitude comparable to its maximum amplitude.

Torrey<sup>5</sup> in subsequent experiments introduced a transient forced precession technique. Although he also observed his output signal while the oscillating com-

ponent of the external field was being applied, he was primarily interested in the transient growth of the nuclear moment at the beginning of a pulse of the oscillating field. The "rapid passage" method introduced by the Bloch group<sup>4</sup> may also be considered a transient forced precession technique.

By pursuing a suggestion which had been made by Bloch,<sup>6</sup> Hahn<sup>7</sup> successfully observed a transient signal or "tail" following the removal of an intense pulse of the oscillating magnetic field. Later, using essentially the same technique, Hahn<sup>8</sup> discovered and explained the "spin echo" effect. Since both "tails" and "echoes" occur when the oscillating field is removed, this is a free precession technique. Furthermore, it is a transient technique since the net nuclear moment undergoes large changes in amplitude. The transient "wiggles" effect<sup>3</sup> may be considered a mixture of free and forced precession.

It is the purpose of this paper to describe an experiment using a steady-state free precession technique and to indicate its special properties. The experimental apparatus used in this experiment is identical to that of the conventional transient free precession equipment with one exception. It is essential that the oscillating rf field be phase coherent from pulse to pulse.

\* This work was partially supported by the Rutgers University Research Council, The Radio Corporation of America, and the United States Air Force Office of Scientific Research, Air Research and Development Command.

<sup>1</sup> Purcell, Torrey, and Pound, *Phys. Rev.* **69**, 37 (1946).

<sup>2</sup> Bloch, Hansen, and Packard, *Phys. Rev.* **69**, 127 (1946).

<sup>3</sup> Bloembergen, Purcell, and Pound, *Phys. Rev.* **73**, 679 (1948).

<sup>4</sup> Bloch, Hansen, and Packard, *Phys. Rev.* **70**, 474 (1946).

<sup>5</sup> H. C. Torrey, *Phys. Rev.* **76**, 1059 (1949).

<sup>6</sup> F. Bloch, *Phys. Rev.* **70**, 460 (1946).

<sup>7</sup> E. L. Hahn, *Phys. Rev.* **77**, 297 (1950).

<sup>8</sup> E. L. Hahn, *Phys. Rev.* **80**, 580 (1950).

## II. MATHEMATICAL ANALYSIS OF THE TECHNIQUE

A mathematical analysis of this experiment will be presented. The reader is encouraged, however, to develop his own qualitative description using a vector model.<sup>8,9</sup> Such a model is helpful in providing a physical understanding of the experiment.

The terminology and notation used by Carr and Purcell<sup>9</sup> will be used for this analysis. The nuclear sample has a total magnetic moment  $\mathbf{M}$ . The magnitude of this total moment under equilibrium conditions in the strong static applied field,  $\mathbf{H} = H_z \mathbf{k}$ , is  $M_0$ .

In describing the precessional motions of the nuclear moments of the sample, it is necessary to take account of the inhomogeneity of the applied field. The fraction of the nuclear moments located in fields having a value within a small interval about  $H_z$  will be denoted by  $f(H_z)dH_z$ . The normalized distribution function  $f(H_z)$  is considered centered at  $H_z = H_{z0}$ . The field deviations from the center of the distribution are  $\delta H_z = H_z - H_{z0}$ . The root-mean-square value of these deviations is designated  $\sigma$ . With each value of  $H_z$  and with an increment  $dH_z$ , there exists an incremental magnetic moment  $d\mathbf{M}(H_z)$ , which is the vector sum of the moments of all nuclei within regions of the sample where the field strength is between  $H_z$  and  $H_z + dH_z$ .

In free precession experiments the oscillating field is applied to the sample in short pulses. For convenience the terminology "radio-frequency" pulses will be used here although in certain low-field experiments the frequency lies in the audio range. The rf magnetic

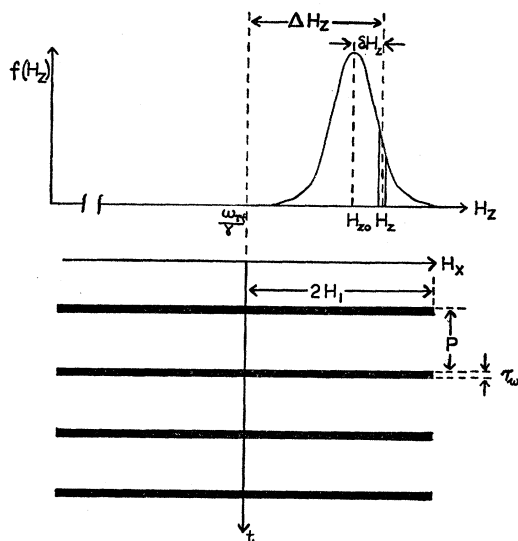


FIG. 1. Relationship of the resonance field  $\omega_{rf}/\gamma$  to the center  $H_{z0}$  of the inhomogeneity distribution  $f(H_z)$  and the field  $H_z$  identifying an increment of nuclear moments. The rf pulses of amplitude  $2H_1$ , width  $\tau_w$ , and spacing  $P$  are represented in the laboratory coordinate system.

<sup>9</sup> H. Y. Carr and E. M. Purcell, Phys. Rev. **94**, 630 (1954).

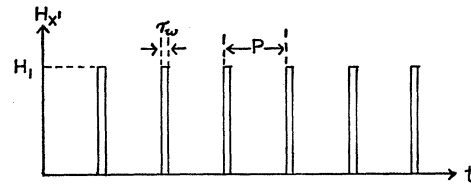


FIG. 2. The rf pulses represented in a coordinate system rotating with the frequency  $\omega_{rf}$ .

field with frequency  $\omega_{rf}$  is applied to the sample at right angles to the strong static field. As is customary, the magnitude of a linearly polarized rf field will be denoted by  $2H_1$ . The static field in which the magnetic moments will have a precessional frequency equal to the frequency of the rf field, is given by  $H_z = \omega_{rf}/\gamma$ , where  $\gamma$  is the gyromagnetic ratio.

In this experiment a steady series of equally spaced rf pulses having equal width and magnitude is applied to the sample. This is indicated schematically in Fig. 1. The pulse width  $\tau_w$  is made small compared with the pulse separation  $P$ . The experiment is best described in a rotating coordinate system<sup>9</sup> (see Fig. 2) whose frequency  $\Omega = -\omega_{rf}\mathbf{k}$  is determined by the frequency of the rf field. It is convenient to choose the phase of the rotating system such that the appropriate rotating component  $H_1$  of the rf field will be along the  $x'$  axis. Thus in the rotating system during a rf pulse, an incremental moment will see an effective field  $\mathbf{H} = \Delta H_z \mathbf{k}' + H_1 \mathbf{i}'$  where  $\Delta H_z = H_z - \omega_{rf}/\gamma$ . In the special case treated by Carr and Purcell,<sup>9</sup>  $\Delta H_z = H_z - H_{z0}$ . Their  $\omega_{rf}$  was not varied but instead had the particular constant value  $\gamma H_{z0}$ .

A nonviscous liquid sample such as water has been used in the initial experiments described in this paper. The well-known Bloch equations provide an adequate description of the dynamic motion of the net magnetic moment for such liquid samples. In order to simplify these equations and their solutions the following notation is introduced:

$$u = \frac{dM_{x'}(H_z)}{dM_0(H_z)}, \quad v = \frac{dM_{y'}(H_z)}{dM_0(H_z)}, \quad m = \frac{dM_{z'}(H_z)}{dM_0(H_z)}. \quad (1)$$

Here the primes refer to the rotating coordinate system and  $dM_0(H_z)$  is the equilibrium value of the net magnetic moment for a given increment. In this notation, the Bloch equations for a particular increment are:

$$\dot{u} = -\frac{u}{T_2} + \gamma v \Delta H_z, \quad (2)$$

$$\dot{v} = -\frac{v}{T_2} - \gamma u \Delta H_z + \gamma m H_{x'}, \quad (3)$$

$$\dot{m} = \frac{1}{T_1}(1-m) - \gamma v H_{x'}. \quad (4)$$

The equatorial components  $u$  and  $v$  decay with a characteristic time constant  $T_2$  while the polar component  $m$  attains its equilibrium value with a characteristic time constant  $T_1$ . During the time  $\tau_w$  that the pulses are on,  $H_{x'} = H_1$ . During the off-time  $P - \tau_w \doteq P$ ,  $H_{x'} = 0$ .

The steady-state nuclear signal in this experiment is determined by the precessing equatorial component of the steady-state nuclear moment. This resultant component is determined from the steady-state values of  $u$  and  $v$  given by the solutions to the above equation. These steady-state values can be determined by assuming  $u$  and  $v$  have the values  $u_0$  and  $v_0$  at the beginning of each period  $P$  after the initial transient of the experiment has died away. Using these initial conditions the solutions to the above equations yield  $u(\tau_w)$ ,  $v(\tau_w)$ ,  $u(P)$ , and  $v(P)$ . By equating the expressions for  $u(P)$  and  $v(P)$  at the end of a period  $P$  to the initial values  $u_0$  and  $v_0$ , the steady-state values may be obtained.

In the present mathematical analysis, the special case of  $H_1 \gg \Delta H_z$  and  $H_1 \gg \sigma$  will be considered. Not

only do these conditions simplify the mathematical solution, but it will be demonstrated that they are necessary conditions for the elimination of the effects of field inhomogeneity on signal strengths. Furthermore, in solving the Bloch equations for the times when the rf pulses are on, it is always assumed that  $\tau_w \ll T_2 \leq T_1$ . The amplitudes of the components undergo very little decay during these times and the terms in the differential equations related to the decay can be neglected. Thus the solution is simply the rapid precession of  $\mathbf{M}$  about the  $x'$  axis for the short time  $\tau_w$ ,

$$\begin{bmatrix} u(t) \\ v(t) \\ m(t) \end{bmatrix} = \begin{bmatrix} 1 & 0 & 0 \\ 0 & \cos \Delta\theta(t) & \sin \Delta\theta(t) \\ 0 & -\sin \Delta\theta(t) & \cos \Delta\theta(t) \end{bmatrix} \begin{bmatrix} u(0) \\ v(0) \\ m(0) \end{bmatrix}, \quad (5)$$

where  $\Delta\theta(t) = \gamma H_1 t$  is the change in the azimuthal angle in the equatorial  $y'-z'$  plane with  $x'$  as polar axis.

For the periods  $P - \tau_w \doteq P$  when the pulses are off, the decay terms cannot be neglected, but  $H_1 = 0$ . The solutions to the Bloch equations are found to involve both precession and decay:

$$\begin{bmatrix} u(t) \\ v(t) \\ m(t) \end{bmatrix} = \begin{bmatrix} \cos \Delta\phi(t) & \sin \Delta\phi(t) & 0 \\ -\sin \Delta\phi(t) & \cos \Delta\phi(t) & 0 \\ 0 & 0 & 1 \end{bmatrix} \begin{bmatrix} u(0)e^{-t/T_2} \\ v(0)e^{-t/T_2} \\ [1 - [1 - m(0)]e^{-t/T_1}] \end{bmatrix}, \quad (6)$$

where  $\Delta\phi(t) = \gamma \Delta H_z t$  is the change in the azimuthal angle in the equatorial plane  $x'-y'$  with  $z'$  as polar axis.

It is the object of the present steady-state experiment to obtain components  $u$ ,  $v$ , and  $m$  which do not change appreciably during the time  $P$  from the values  $u_0$ ,  $v_0$  and  $m_0$ . This is possible by making  $P \ll T_2 \leq T_1$ . Furthermore, in this initial analysis it is assumed that  $T_1 \doteq T_2 \doteq T$ . This is an adequate approximation for non-viscous samples such as liquid water. With these conditions, the steady-state solutions are

$$u \doteq u_0 = [\cot \frac{1}{2} \Delta\theta (\sin \frac{1}{2} \Delta\phi \cos \frac{1}{2} \Delta\phi)] / \Lambda, \quad (7)$$

$$v \doteq v_0 = -(\cot \frac{1}{2} \Delta\theta \sin \frac{1}{2} \Delta\phi) / \Lambda, \quad (8)$$

$$m \doteq m_0 = (\cot^2 \frac{1}{2} \Delta\theta \sin^2 \Delta\phi), \quad (9)$$

where  $\Lambda = 1 + (\cot \frac{1}{2} \Delta\theta \sin \frac{1}{2} \Delta\phi)^2$ . If the detector is sensitive only to amplitude, the nuclear signal will be directly proportional to the amplitude of the resultant equatorial component. This is

$$w \doteq w_0 = (u_0^2 + v_0^2)^{\frac{1}{2}} \doteq \frac{\cot \frac{1}{2} \Delta\theta \sin \frac{1}{2} \Delta\phi}{1 + (\cot \frac{1}{2} \Delta\theta \sin \frac{1}{2} \Delta\phi)^2}. \quad (10)$$

Here  $\Delta\theta$  is determined by  $H_1$  and  $\tau_w$  while  $\Delta\phi$  is determined by  $\Delta H_z$  and  $P$ ; that is,  $\Delta\theta = \gamma H_1 \tau_w$  and  $\Delta\phi = \gamma \Delta H_z P$ .

The solution for  $w$  is periodic in  $\Delta\phi$ , vanishing whenever  $\frac{1}{2} \Delta\phi = \frac{1}{2} \gamma \Delta H_z P = 2n\pi$ , where  $n$  is any integer. Since  $\Delta H_z = H_z - \omega_{rf} / \gamma$ , this periodicity can be observed by varying  $P$ ,  $H_z$ , or  $\omega_{rf}$ . Between the null points, the

signal has a form similar to that of a dispersion curve. The amplitude, however, is positive on both sides of the nulls. In Fig. 3 the signal has been plotted as a function of  $\Delta\phi$  for six values of  $\Delta\theta$ . The width of the dispersion curve is determined by  $\Delta\theta$ . The first peaks occur at  $\tan \frac{1}{2} \Delta\phi = \sin \frac{1}{2} \Delta\theta$  for  $\Delta\theta \leq 90^\circ$ , and at  $\Delta\phi = \pi$  for  $90^\circ \leq \Delta\theta < 180^\circ$ . The peak value is  $\frac{1}{2}$  for  $\Delta\theta \leq 90^\circ$ .

There is a null point at the center of the response where  $\omega_{rf} = \gamma H_z$ . It is possible, however, to shift the entire response by  $180^\circ$  in  $\Delta\phi$ . This is done by providing alternate rf pulses with a  $180^\circ$  shift in phase. For these alternate pulses  $H_{x'} = -H_1$ . In this case, there will be a peak at the center of the response when  $\Delta\theta \geq 90^\circ$ . It is not difficult to use the vector model to illustrate

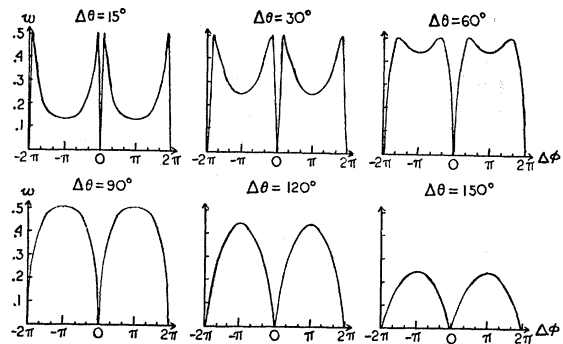


FIG. 3. The steady-state free precession response  $w$  plotted as a function of  $\Delta\phi = \gamma \Delta H_z P$  as predicted by Eq. (10). Six different values of  $\Delta\theta = \gamma H_1 \tau_w$  are illustrated.

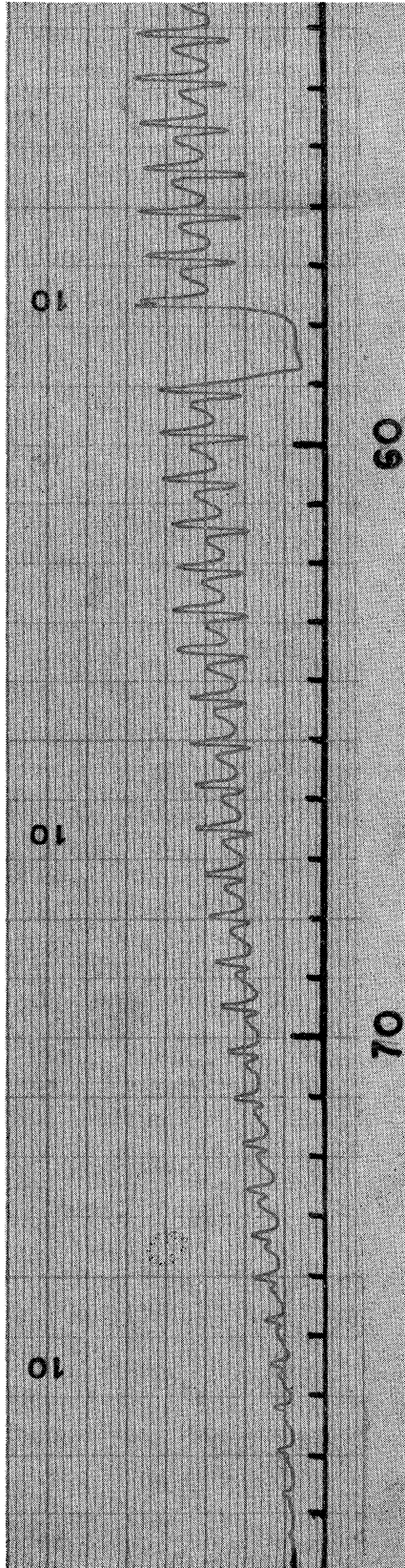


FIG. 4. (a)

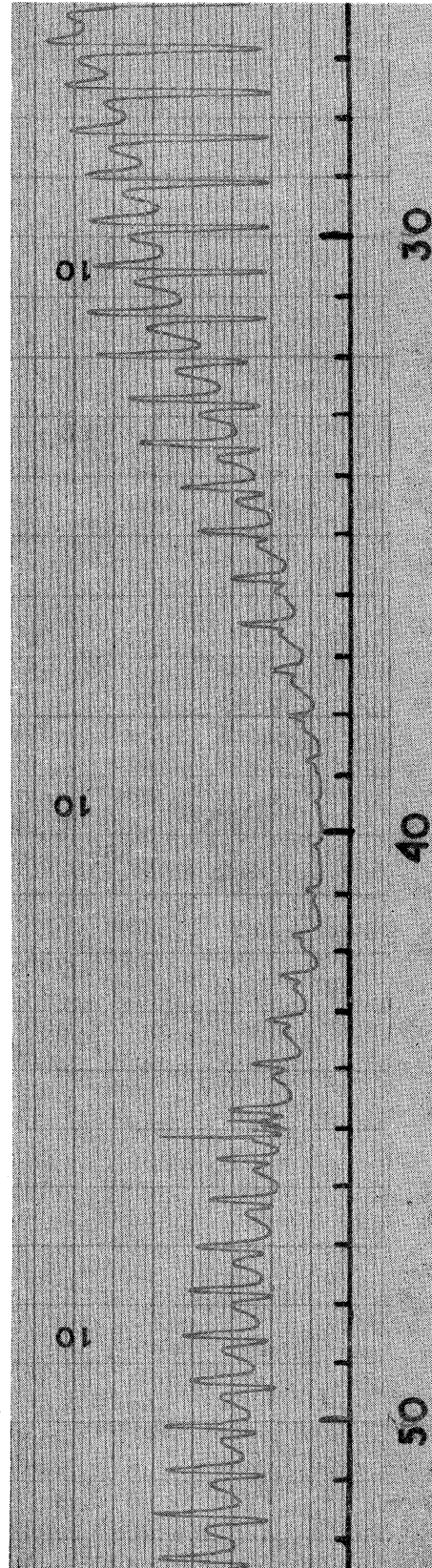


FIG. 4. (b)

FIG. 4. Photograph of a steady-state free precession response from a glycerine sample using an amplitude-sensitive detector and strip chart recorder. As a function of time the response moves from right to left. Each marker corresponds to 10 sec and 0.31 gauss. The pulse repetition frequency is 1000 cps and the pulse width is approximately 20 μsec. [Figure 4(c) is on next page.]

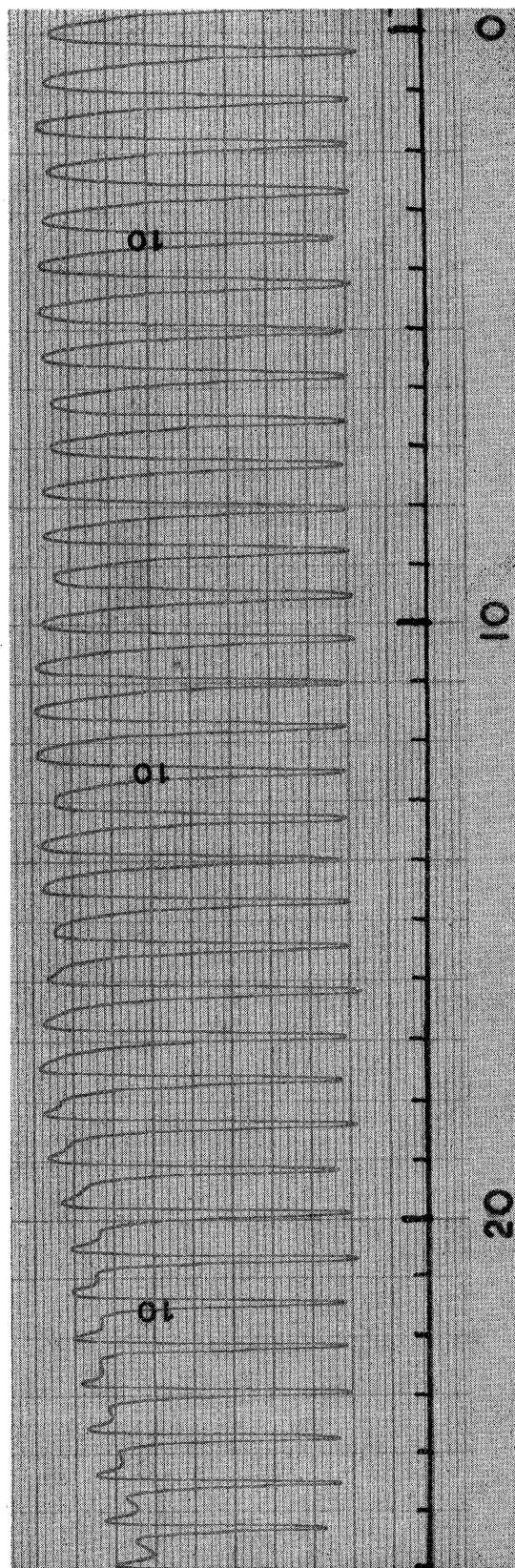


FIG. 4. (c)

qualitatively the differences between these two versions of the experiment.

### III. SPECIAL PROPERTIES OF THE TECHNIQUE

This technique possesses the general properties of steady-state and free precession techniques. A steady-state signal can be observed with a narrow-band detector, thus improving the signal-to-noise ratio. There generally is no need in a free precession experiment for a bridge or other similar device to buck out the externally applied rf signal while observing the weak nuclear signal. However, if a large number of pulses is used, it may be useful to devise a method to buck out the signal caused by the pulses alone.

This technique has two special properties which should be noted. One involves the band width of the response and the other the effect of the inhomogeneity of the magnet. It is possible in this experiment to obtain a nuclear signal over a wide range of frequencies or magnetic fields. The upper limit to this wide-band response is determined not by the nuclear sample or the magnet, but by the electronic equipment. In many situations electronic equipment is varied more easily than the properties of the magnet or the sample. To obtain a response at larger values of  $\Delta H_z$ , one simply increases the power of the rf pulse amplifier sufficiently to insure that  $H_1$  always remains much larger than the desired  $\Delta H_z$ . Frequently a wide-band response is a disadvantage, but in certain applications this may be an advantage. One example might be the search for an unknown resonance.

This over-all broad response may contain fine structure. Equation (10) indicates that for very small values of  $\Delta\theta$ , the width  $\Delta\phi$  from the nulls to the peaks of the dispersion structure is equal to  $\Delta\theta$ . Thus if  $P$  is kept constant, the peaks come at smaller values of  $\Delta H_z$  as  $\Delta\theta$  is decreased. It is not possible, of course, to use this technique to obtain an infinitely narrow response. The natural relaxation time of the incremental samples places a lower limit on the width. Equation (10) was derived on the assumption that  $(\Delta\theta)T/P \geq 1$ . For a given  $T$  and a small  $\Delta\theta$  this implies that  $P$  must be small; that is, in the limit of small  $\Delta\theta$  there must be a large number of pulses within one relaxation time. The band width of the dispersion curve is dependent on the value of  $P$ . At the first peaks,  $\Delta H_z = \Delta\phi/\gamma P \approx \Delta\theta/\gamma P$ . But in the limiting case  $P \approx (\Delta\theta)T$ , this width becomes  $\Delta H_z = 1/\gamma T$ . This is the natural line width of the nuclear sample.

Finally, this technique possesses an important property similar to that of the "spin echo." The effect of the inhomogeneity of the magnetic field on signal strength can be eliminated under certain conditions. Equation (10) represents the solution of the Bloch equations for one increment of the sample. This is the fraction  $f(H_z)dH_z$  located in the field  $H_z$ . The effect of



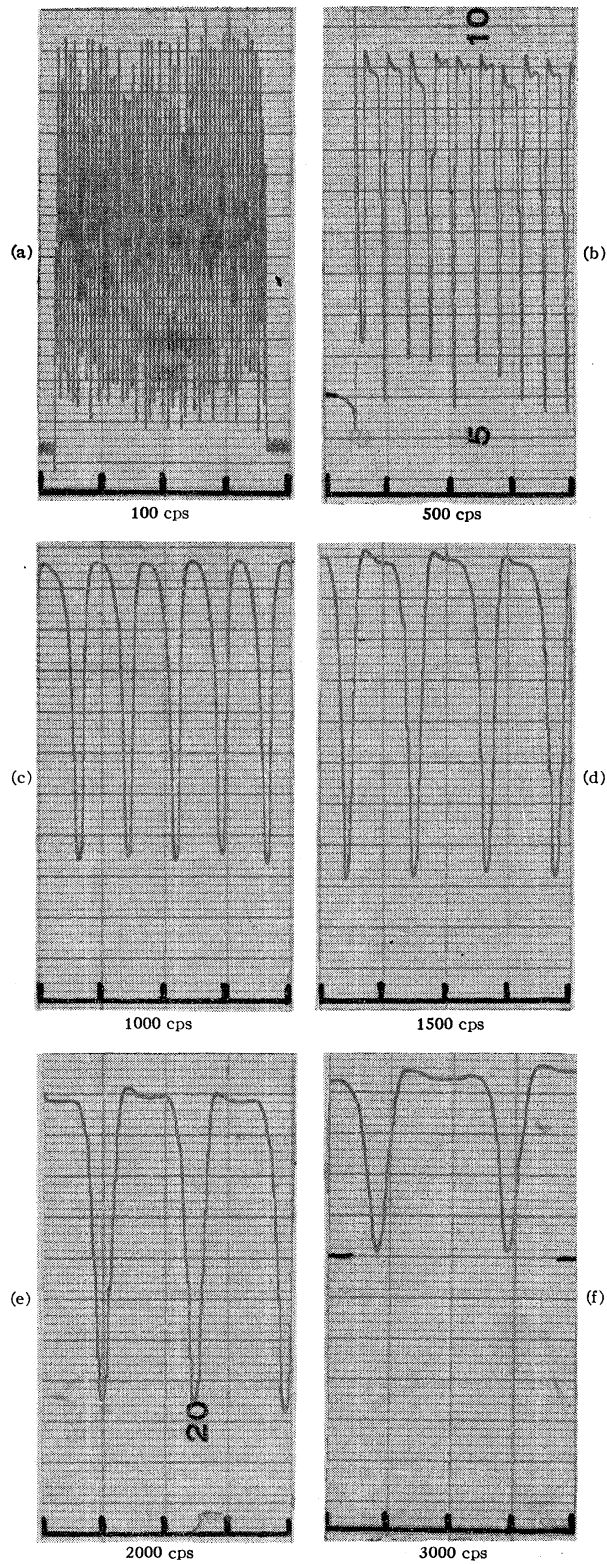


FIG. 5. Photograph of the central portion of a steady-state free precession response as a function of pulse repetition frequency. Time markers correspond to 10 sec or 0.31 gauss, and  $\Delta\theta = 90^\circ$ .

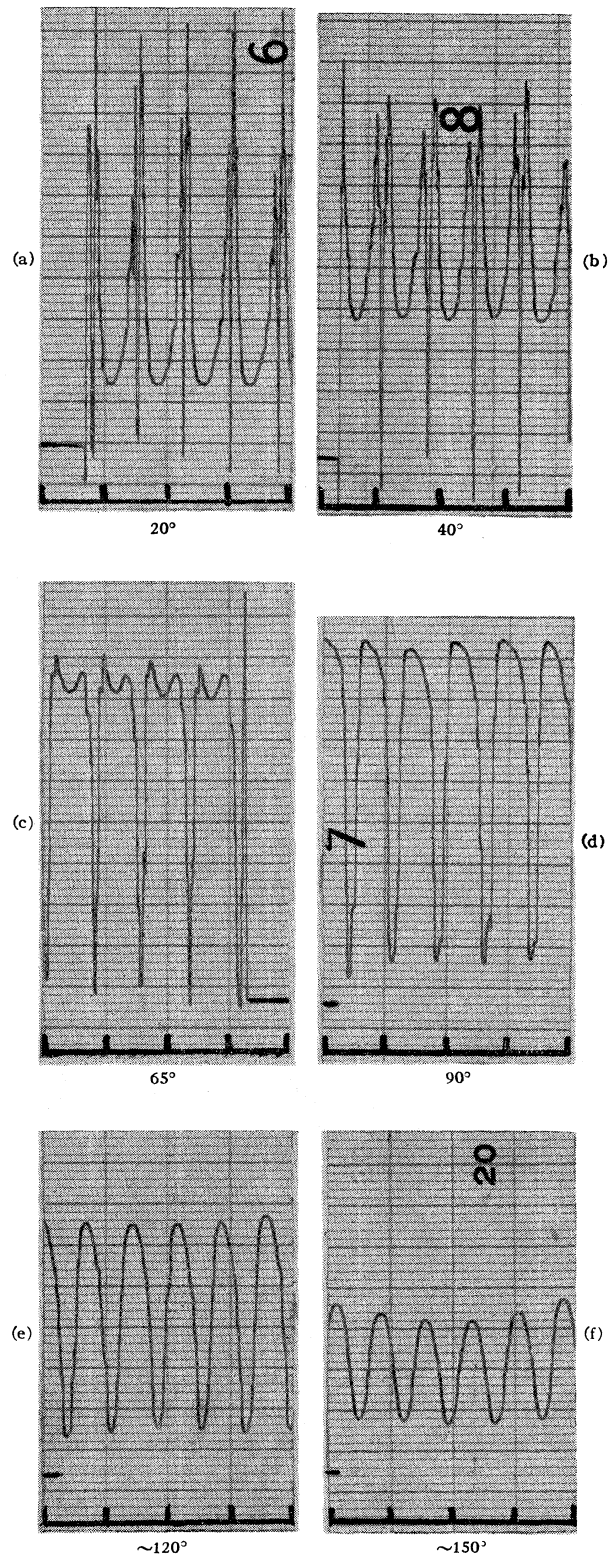


FIG. 6. Photograph of the central portion of a steady-state free precession response as a function of  $\Delta\theta = \gamma H_1 \tau_w$ . The pulse repetition frequency is 1000 cps and the markers correspond to 10 sec or 0.31 gauss. Time increases to the left.

the inhomogeneity enters as one integrates over the entire sample to determine the equatorial component  $W$  of the total magnetic moment. This is accomplished by multiplying Eqs. (7) and (8) by  $f(H_z)$  and integrating each over all values of  $H_z$ :

$$U \doteq U_0 = \int u_0 f(H_z) dH_z, \quad (11)$$

$$V \doteq V_0 = \int v_0 f(H_z) dH_z. \quad (12)$$

The total signal from the sample is determined by the magnitude of the resultant:

$$W \doteq W_0 = (U_0^2 + V_0^2)^{\frac{1}{2}}. \quad (13)$$

For values of  $\Delta\theta \doteq 1$  the widths of the factors  $u_0$  and  $v_0$  in Eqs. (11) and (12) are the order of  $1/\gamma P$ . Thus if one makes  $1/\gamma P$  much larger than the width  $\sigma$  of  $f(H_z)$ , the inhomogeneity distribution acts like a delta function and  $U$  and  $V$  are identical to  $u_0$  and  $v_0$  with  $H_z$  replaced by  $H_{z0}$ . Thus the response is as though all moments were situated in the field  $H_{z0}$ ; that is, as though the effect of the inhomogeneity had been eliminated. The above condition can be expressed in terms of a decay time  $T_2^* \doteq 1/\gamma\sigma$  associated with the static inhomogeneity. To eliminate the effect of the inhomogeneity on signal strength one must make  $P \ll T_2^*$ .

It is of interest to ask if one can obtain simultaneously both a large signal strength and a narrow dispersion curve band width. The answer is that this is impossible. For small values of  $\Delta\theta$ ,  $W$  is determined by  $U_0$ . But the form of  $U_0$  is determined by the factor  $u_0$  which for small values of  $\Delta\theta$  has a width the order of  $\Delta\theta/\gamma P$ . Thus the necessary condition for eliminating the effect of the inhomogeneity of the magnet on signal strength is  $\Delta\theta/\gamma P \gg 1/\gamma T_2^*$ . If, in an effort to obtain a narrow band width,  $\Delta\theta/\gamma P$  becomes smaller than  $1/\gamma T_2^*$ , then the response will be determined by  $f(H_z)$  instead of  $u_0$ . In this case the effect of the inhomogeneity on signal strength is not eliminated. This question may be approached in an alternate way. It was shown above that for a given increment the dispersion response can have the natural line width  $1/\gamma T$ . This corresponds to the smallest possible  $\Delta\theta \doteq P/T$ . If the field is inhomogeneous, then to obtain a steady state involving the maximum signal contributed by all increments, the smallest  $\Delta\theta$  one can allow is the order of  $P/T_2^*$ . The line width will be  $1/\gamma T_2^*$ . Thus the lower limit to the width of the dispersion curve in this case is again seen to be determined by the inhomogeneity of the magnet. A nuclear sample in a very homogeneous external field but possessing a complex distribution function  $f(H_z)$  due to local chemical shifts, should reflect the chemical shift structure in the response pattern near the nulls.

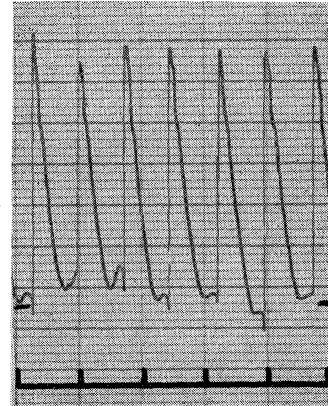


FIG. 7. Photograph of the central portion of a steady-state free precession response from an oxygen-free water sample with  $T_1 \doteq 3.5$  sec. The effect of a sweep time comparable to the relaxation time is illustrated. Time increases to the left. Each marker indicates 10 sec.

In summary, this free precession technique, unlike the transient free precession technique, provides a steady-state signal which can be detected with a narrow-band receiver thus improving the sensitivity. Furthermore, this steady-state technique, unlike the steady-state forced precession technique, provides a free precession response in which the effect of inhomogeneity of the magnet on signal amplitude can be eliminated. Finally, the technique provides a very wide-band response which may be useful, for example, in searching for unknown resonances or in applications in which a large number of side bands are desired.

#### IV. EXPERIMENTAL RESULTS

Exploratory experiments utilizing this technique have been carried out in this laboratory. The phase-coherent

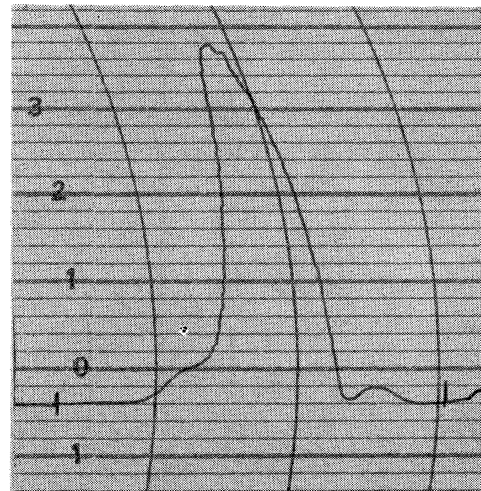


FIG. 8. Photograph of the steady-state free precession response obtained using a strip chart recorder with time constant long compared to the time used to sweep through a null in the dispersion structure. The fine structure of Fig. 4 is averaged out.

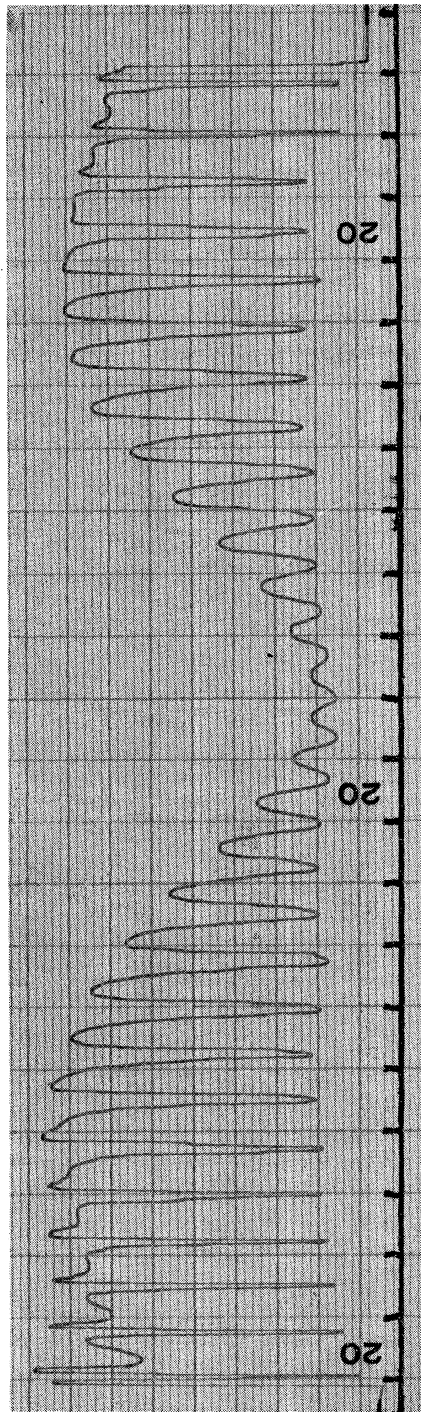


Fig. 9. Photograph of the central portion of a steady-state free precession response for  $\Delta\theta \doteq 180^\circ$ . As  $\Delta H_z$  assumes values comparable to  $H_1$ , the  $180^\circ$  condition no longer exists. The markers represent 0.31 gauss and  $H_1 \doteq 3$  gauss.

rf pulses were obtained by feeding the output of a General Radio Oscillator, Model No. 1001, into a gated tuned amplifier similar to that used by Dicke and Romer.<sup>10</sup> The remainder of the equipment is equivalent to that of any conventional free precession experiment.<sup>8,11,12</sup>

The third picture in Fig. 4 is a photograph of one-half of the central portion of a strip chart recording of the detected nuclear signal as the magnetic field  $H_z$  was varied. The center of the resonance is located at the right edge of the picture. Transient free precession techniques initially were used to set  $\Delta\theta$  at approximately  $90^\circ$ .  $P$  is equal to 0.001 sec and  $\tau_w \doteq 20 \mu\text{sec}$ . Since the signal is from protons in glycerine ( $\gamma = 2.68 \times 10^4$ ), the separation between nulls is approximately 0.235 gauss and  $H_1 \doteq 3$  gauss. The inhomogeneity over the sample is  $\sigma \doteq 0.01$  gauss.

The photographs in Fig. 5 illustrate the dependence of the central portion of the response on the pulse frequency. The field spacing between nulls varies directly with the pulse repetition frequency as predicted in Eq. (10). The inhomogeneity for Fig. 5 corresponds to  $\sigma \doteq 0.003$  gauss.

The photographs in Fig. 6 record an experimental verification of the dependence of the response on  $\Delta\theta$  predicted in Eq. (10). The pulse widths used in the experiments recorded in Fig. 6 are very close to those used in the theoretical plots given in Fig. 3. In these experiments  $\Delta\theta$  was changed by varying  $\tau_w$ .

Particularly in those pictures where the amplitude is large, the photographs do not have precisely the predicted symmetry about the nulls. This can be attributed to a sweep rate which is not slow compared to the relaxation times. The steady state is not attained. Since the time record is progressing from right to left one expects the peaks to the right of a null to be larger than those to the left. This effect is clearly illustrated in Fig. 7. Here an oxygen-free water sample ( $T_1 \doteq 3.5$  sec) was substituted for the glycerine ( $T_1 \doteq 0.05$  sec). The saw-toothed response results from the failure to reach a steady state during the signal growth determined by  $T_1$ . On the other hand, a complete steady state is attained during the signal decay which is determined by  $T_2^* \ll T_1$ .

Another effect is illustrated in the photograph of Fig. 8. Here a glycerine sample is used, but the response time of the recorder is made so long that the fine structure of Fig. 4 is averaged out. It is not difficult to obtain such response curves 10 gauss wide, even though a liquid with its very narrow natural line width is used as the sample.

<sup>10</sup> R. H. Dicke and R. H. Romer, Rev. Sci. Instr. **26**, 915 (1955).

<sup>11</sup> J. Schwartz, Rev. Sci. Instr. **28**, 780 (1957).

<sup>12</sup> Buchta, Gutowsky, and Woessner, Rev. Sci. Instr. **29**, 55 (1958).



The "off-resonance" shape of a steady-state free precession response is illustrated in the top two pictures of Fig. 4. An appreciable signal is detected as far out as approximately 65 markers (20 gauss) from the center of the response. The sample was removed from the rf coil between the 58th and 59th markers in order to determine the zero signal level. In the second picture an envelope minimum is observed at the 40th marker or approximately 12 gauss from the center of the response. This response minimum comes at a position given by a null in the frequency distribution of a single pulse of width  $\tau_w$ . This is at the field  $\Delta H_z = 2N\pi/\gamma\tau_w$  where  $N=1$ . Similarly, a Fourier analysis of a series of such pulses equally spaced with a period  $P$  can be used to

describe the fine-structure nulls within the envelope of the response.

In general, as one moves away from the center of the response to a value of  $H_z$  comparable to  $H_1$ , the effective value of  $\Delta\theta$  is altered. The effective value of  $\Delta\theta$  is defined by comparison with the shapes shown in Fig. 6. Figure 4 illustrates this point for  $\Delta\theta = 90^\circ$  at the center of the response. Figure 9 does the same for  $\Delta\theta = 180^\circ$ . In the latter case the effective value of  $\Delta\theta$  appears to be less than  $90^\circ$  at about 10 markers or approximately 3 gauss from the center of the response. This illustrates that the  $180^\circ$  pulse adjustment is more sensitive than a  $90^\circ$  pulse adjustment, a fact also very basic to transient free precession adjustments.

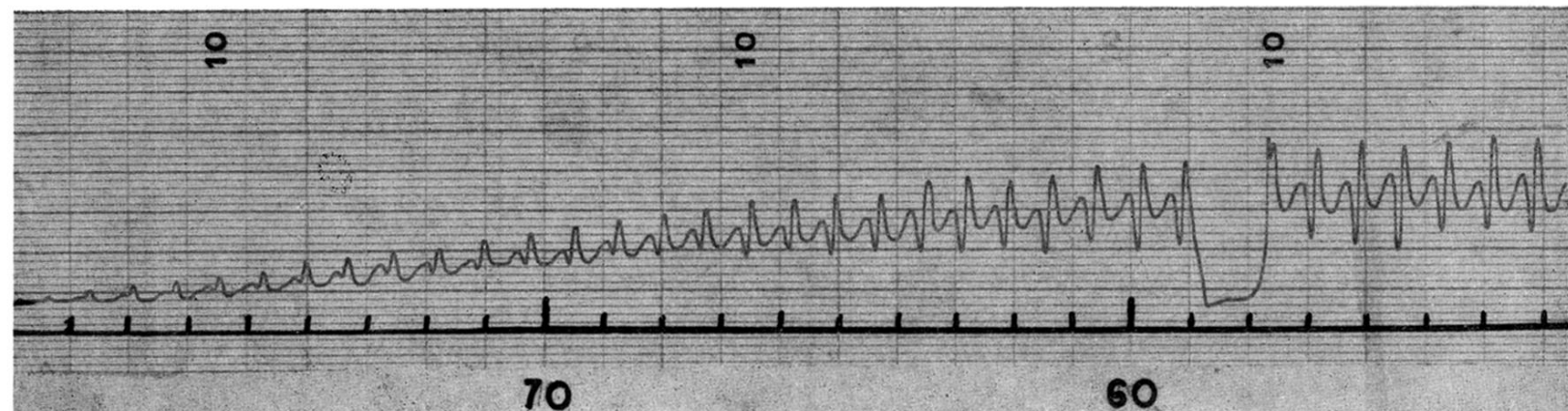


FIG. 4. (a)

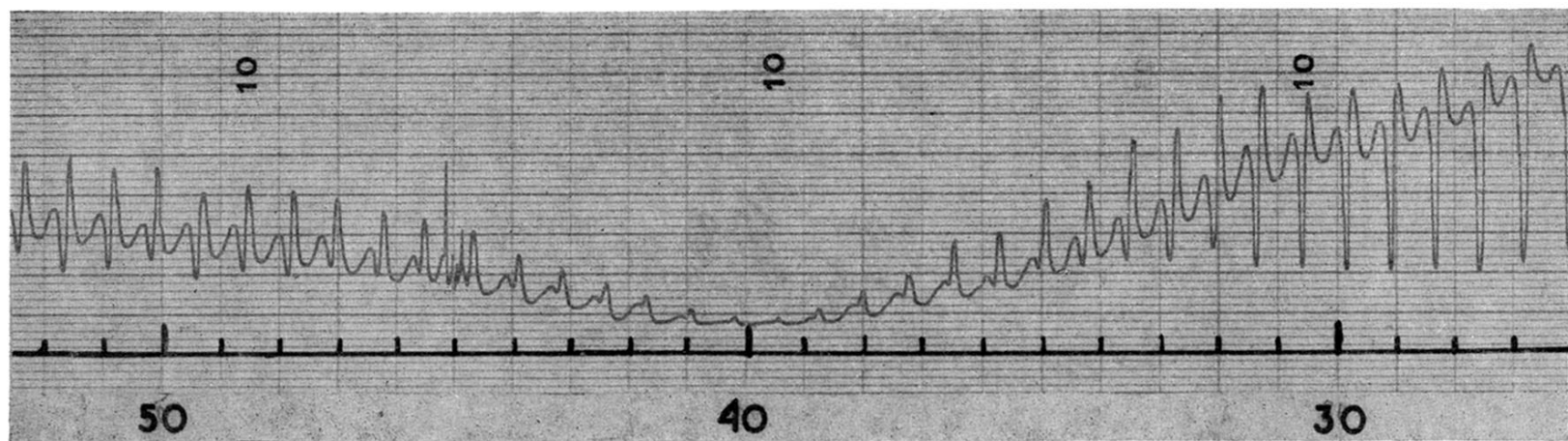


FIG. 4. (b)

FIG. 4. Photograph of a steady-state free precession response from a glycerine sample using an amplitude-sensitive detector and strip chart recorder. As a function of time the response moves from right to left. Each marker corresponds to 10 sec and 0.31 gauss. The pulse repetition frequency is 1000 cps and the pulse width is approximately 20  $\mu$ sec. [Figure 4(c) is on next page.]

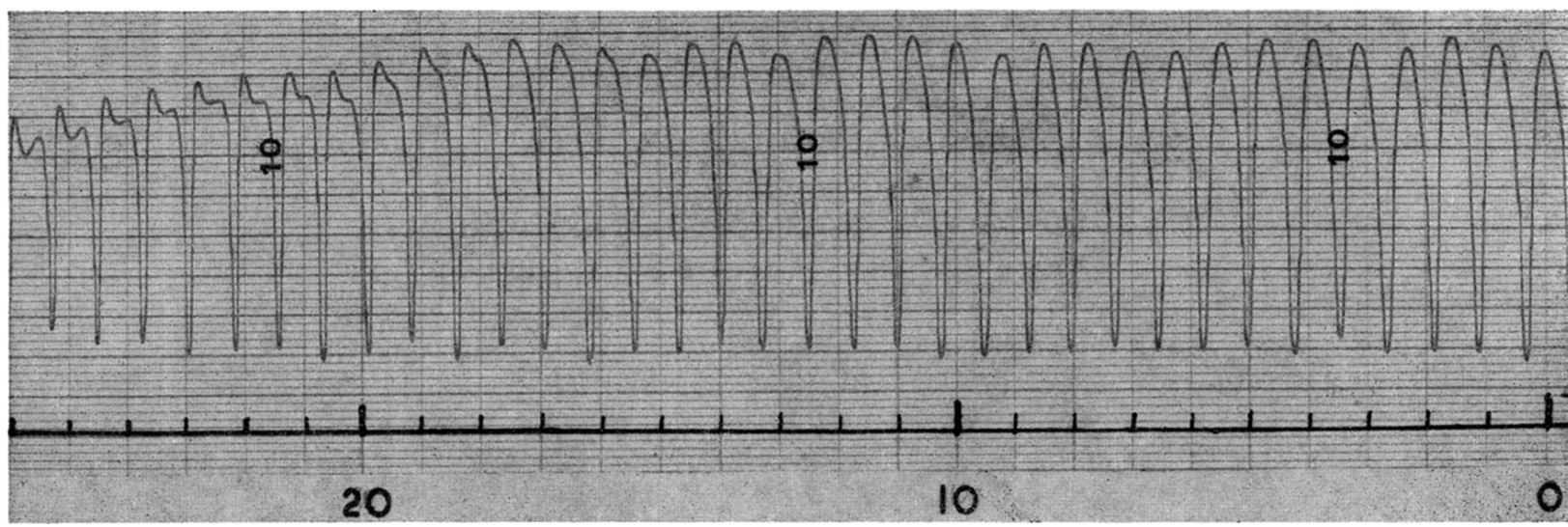


FIG. 4. (c)

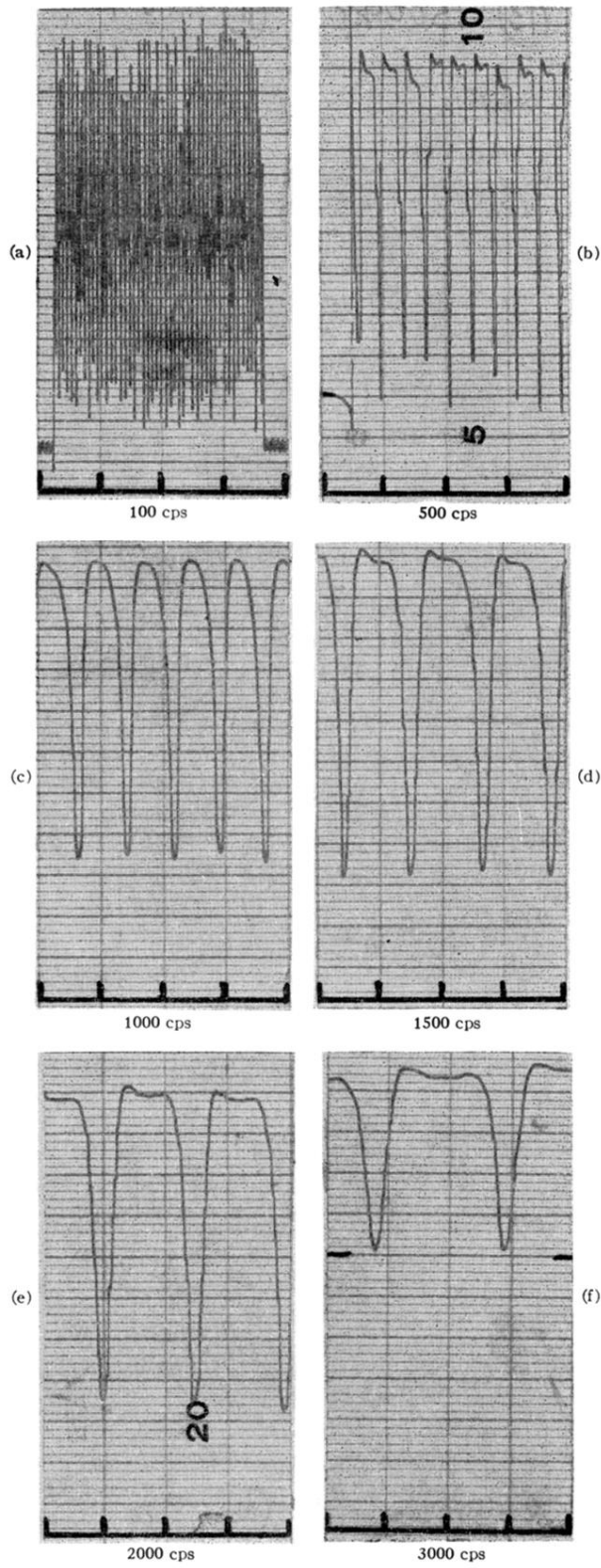


FIG. 5. Photograph of the central portion of a steady-state free precession response as a function of pulse repetition frequency. Time markers correspond to 10 sec or 0.31 gauss, and  $\Delta\theta = 90^\circ$ .



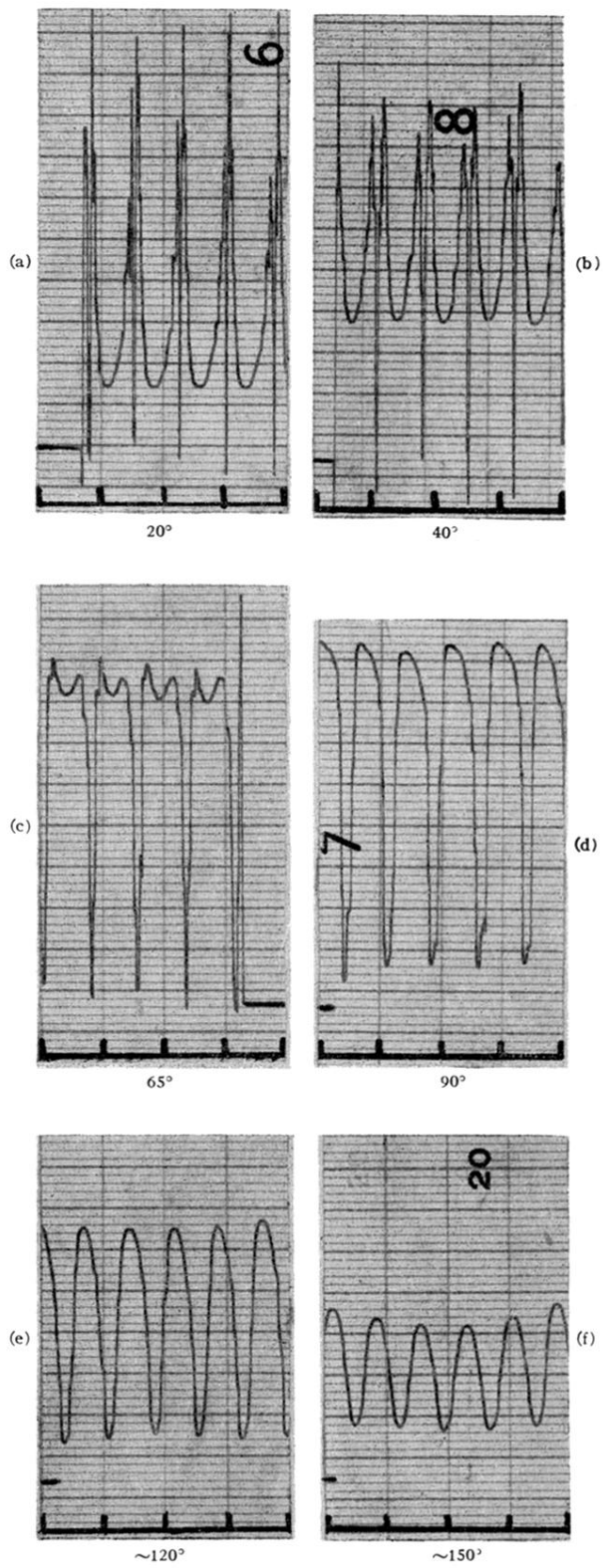


FIG. 6. Photograph of the central portion of a steady-state free precession response as a function of  $\Delta\theta = \gamma H_1 \tau_w$ . The pulse repetition frequency is 1000 cps and the markers correspond to 10 sec or 0.31 gauss. Time increases to the left.

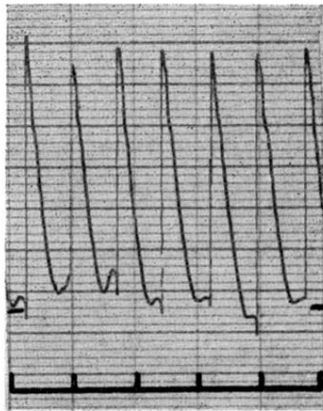


FIG. 7. Photograph of the central portion of a steady-state free precession response from an oxygen-free water sample with  $T_1 \approx 3.5$  sec. The effect of a sweep time comparable to the relaxation time is illustrated. Time increases to the left. Each marker indicates 10 sec.

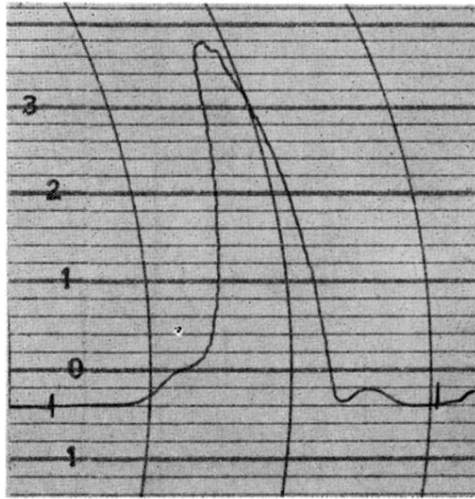


FIG. 8. Photograph of the steady-state free precession response obtained using a strip chart recorder with time constant long compared to the time used to sweep through a null in the dispersion structure. The fine structure of Fig. 4 is averaged out.

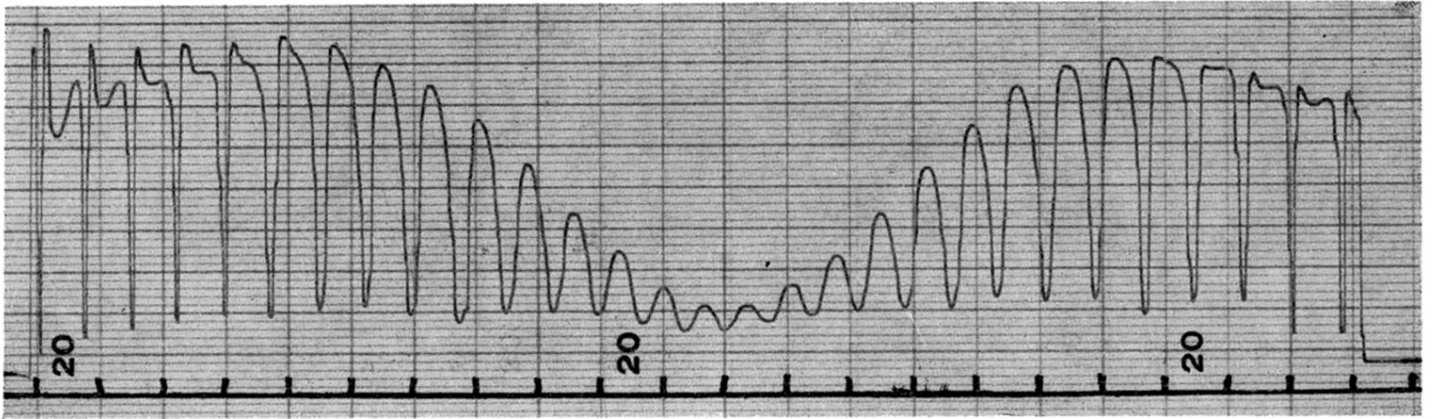


FIG. 9. Photograph of the central portion of a steady-state free precession response for  $\Delta\theta \doteq 180^\circ$ . As  $\Delta H_z$  assumes values comparable to  $H_1$ , the  $180^\circ$  condition no longer exists. The markers represent 0.31 gauss and  $H_1 \doteq 3$  gauss.